Magnetoresistance, Anisotropic

The electrical conductivity of spontaneously magnetized materials depends on the relative orientation of the electrical current and the magnetization. This phenomenon, called anisotropic magnetoresistance (AMR) or spontaneous magnetoresistance anisotropy (SMA), was discovered by Lord Kelvin in the middle of the nineteenth century. However, intensive investigations on AMR started only in the 1950s with the work of Smit (1951) and van Elst (1959). Although technical applications of AMR were suggested in the 1970s, corresponding devices (sensors and read heads for hard disks) (Göpel *et al.* 1989) were not introduced commercially until about 20 years later. The physical origin of AMR is the reduction of the symmetry of a magnetized material compared to its nonmagnetic state caused by the simultaneous presence of the magnetization and spin–orbit coupling. The first qualitative models to describe AMR were developed by Smit (1951) and Campbell *et al.* (1970) and have been extended subsequently by others. A parameter-free theoretical description of AMR has been published (Banhart and Ebert 1995).

1. *Phenomenological Description*

For a material that is homogeneously magnetized along the z-axis but otherwise isotropic, the conductivity tensor takes the following form (Kleiner 1966, Cracknell 1973):

$$\boldsymbol{\sigma} = \begin{pmatrix} \sigma_\perp & \sigma_H & 0 \\ -\sigma_H & \sigma_\perp & 0 \\ 0 & 0 & \sigma_\parallel \end{pmatrix} \tag{1}$$

with the corresponding resistivity tensor being given by

$$\boldsymbol{\rho} = \begin{pmatrix} \rho_\perp & \rho_H & 0 \\ -\rho_H & \rho_\perp & 0 \\ 0 & 0 & \rho_\parallel \end{pmatrix} \tag{2}$$

The tensor elements $\rho_\perp$ and $\rho_\parallel$ are called transverse and longitudinal electrical resistivity, respectively, with their average

$$\bar{\rho} = \tfrac{2}{3}\rho_\perp + \tfrac{1}{3}\rho_\parallel \tag{3}$$

giving the isotropic resistivity $\bar{\rho}$. Normalizing $\rho_\perp$ and $\rho_\parallel$ using $\bar{\rho}$ leads to the transverse and longitudinal magnetoresistivity, respectively:

$$\left(\frac{\Delta\rho}{\bar{\rho}}\right)_\perp = \frac{\rho_\perp - \bar{\rho}}{\bar{\rho}} \tag{4}$$

$$\left(\frac{\Delta\rho}{\bar{\rho}}\right)_\parallel = \frac{\rho_\parallel - \bar{\rho}}{\bar{\rho}} \tag{5}$$

The difference of these two quantities gives the AMR ratio

$$\frac{\Delta\rho}{\bar{\rho}} = \frac{\rho_\parallel - \rho_\perp}{\bar{\rho}} \tag{6}$$

The off-diagonal element ρ_H of the resistivity tensor is called the Hall resistivity and represents the anomalous or spontaneous Hall effect (Karplus and Luttinger 1954, Smit 1955). The elements of the conductivity tensor $\boldsymbol{\sigma}$ are denoted in an analogous way to those of the resistivity tensor $\boldsymbol{\rho}$ with the following relationships between the various elements:

$$\sigma_\perp = \frac{\rho_\perp}{\rho_\perp^2 + \rho_H^2} \quad \sigma_\parallel = \frac{1}{\rho_\parallel} \quad \sigma_H = \frac{\rho_H}{\rho_\perp^2 + \rho_H^2} \tag{7}$$

$$\rho_\perp = \frac{\sigma_\perp}{\sigma_\perp^2 + \sigma_H^2} \quad \rho_\parallel = \frac{1}{\sigma_\parallel} \quad \rho_H = \frac{\sigma_H}{\sigma_\perp^2 + \sigma_H^2} \tag{8}$$

2. *Basic Properties*

In principle, the above definitions apply to a single-domain sample. For a multidomain sample one therefore has to apply an external magnetic field to align the magnetization. This may lead, for example, to a variation of $\rho_\perp$ and $\rho_\parallel$ with the field, as shown in Fig. 1 (van Elst 1959). Because the ordinary magnetoresistance is superimposed onto the spontaneous magneto-resistance the proper values $\rho_\perp^0$ and $\rho_\parallel^0$, corresponding to the single-domain state of the sample are obtained by an extrapolation of the high-field data to zero external field.

The simple form given above for the conductivity and resistivity tensors is not restricted to isotropic materials, but applies to any material for which the direction of the magnetization coincides with an at least three-fold rotational symmetry axis (Kleiner 1966, Cracknell 1973). Furthermore, it can be applied without modifications for polycrystalline materials. For less symmetric situations the shape of the tensors in Eqns. (1) and (2) will change. In particular, for single crystals one finds that the AMR varies if the orientation of the magnetization with respect to the crystal axis is changed (Becker and Döring 1939).

3. *Materials and Applications*

The AMR effect can be observed in principle in any spontaneously magnetized material. However, most experimental work has been devoted to systems based on the transition metals iron, cobalt, and nickel. In the search for materials with high AMR ratio, diluted and concentrated alloys among these elements, but also with other transition metals (e.g., chromium, vanadium, copper, palladium, and platinum) or non-transition elements (e.g., aluminum, silicon, tin) have

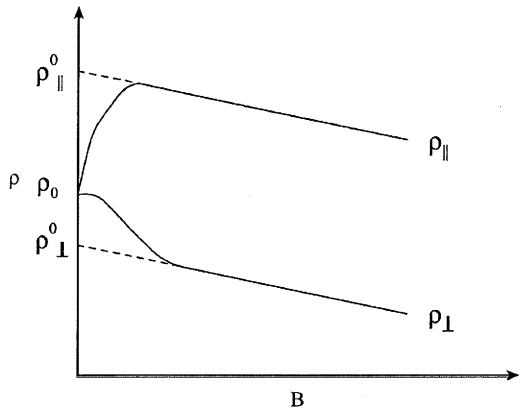

Figure 1
Dependency of the transverse and longitudinal electrical resistivity, $\rho_{\perp}$ and $\rho_{\parallel}$, respectively, on an external magnetic field, B.

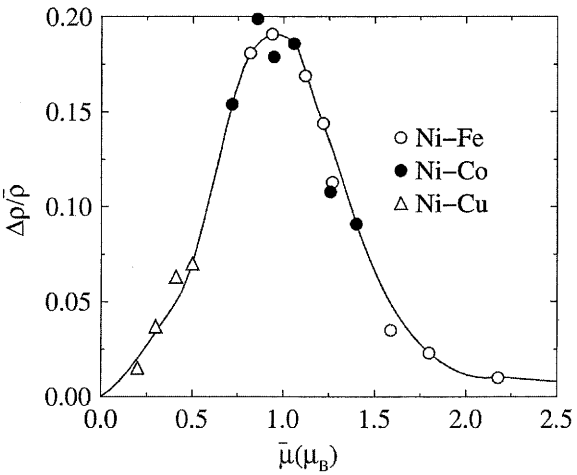

Figure 2
AMR ratio $\Delta\rho/\bar{\rho}$ at 20K as a function of the average magnetic moment $\bar{\mu}$ for various 3d element alloys (after Wijn 1991).

been investigated (McGuire and Potter 1975, Dorleijn 1976). Among these systems the highest values for the AMR ratio $\Delta\rho/\bar{\rho}$ have been found for nickel-based alloys. In particular, a rather simple empirical relationship between the AMR ratio $\Delta\rho/\bar{\rho}$ and the average magnetic moment μ has been found for concentrated binary nickel-based alloys (see Fig. 2 and below). This relationship implies that the AMR ratio can be optimized within certain limits by a suitable choice of the alloy partners and their concentration. An upper limit seems to be given by the data for NiCo alloys and NiFeCo alloys, which show AMR ratios of up to 30% at low temperatures. Unfortunately, the AMR ratio rapidly decreases with increasing temperature. For example, for $Ni_{81}Fe_{19}$ one has $\Delta\rho/\bar{\rho} = 20\%$ at $T = 20$K, but only about 3% at $T = 300$K.

The AMR effect has also been investigated for a number of amorphous alloy systems, e.g., Fe–Si, Fe–Zr, and Fe–V–B. These amorphous systems are attractive because they can be easily prepared as thin films by various techniques and because their isotropic resistivity $\bar{\rho}$ is in general almost temperature independent (see *Amorphous Intermetallic Alloys: Resistivity*). Unfortunately, $\bar{\rho}$ is normally quite high (of the order of 100μΩcm) leading to AMR ratios that are usually not much higher than 1%. In contrast to this property of transition metal-based amorphous systems, a very pronounced AMR effect with $\Delta\rho/\bar{\rho}$ up to 26% at low temperature has been found for ferromagnetic amorphous alloys based on uranium and antimony (Freitas and Plaskett 1990). This finding can be ascribed to the strong spin–orbit coupling of uranium (see below).

Although the maximum AMR ratio that can be achieved at room temperature is relatively small, it is nevertheless high enough to be exploited in sensor and storage technology (Göpel *et al.* 1989). Transition metal alloys are very suitable for this purpose, because they can easily be prepared by evaporation or sputtering deposition as thin films. In some cases the resistivity $\bar{\rho}$ of such films can be decreased by up to 30% by tempering. This increases the AMR ratio accordingly leading to a higher output signal for a given input power (Butherus and Nakahara 1985). Further important restrictions for applications are a low magnetostriction and a small coercivity field. These requirements are extremely well fulfilled by permalloy that is free of magnetostriction at 81 at.% nickel. In addition, it has at this composition a very low coercivity field of about $100\,A\,m^{-1}$ and a low uniaxial anisotropy energy constant of about $200\,J\,m^{-3}$. Although the AMR ratio for the NiFe-alloy system is highest for about 90 at.% nickel and although higher values for $\Delta\rho/\bar{\rho}$ are achieved by other transition metal alloy systems (see above), these suitable properties make $Ni_{81}Fe_{19}$ permalloy the most commonly used AMR material for applications. According to this situation, industrial research and development aims to optimize the geometry and readout technique of AMR devices instead of searching for more efficient AMR materials (Eijkel and Fluitman 1990).

4. *Phenomenological Theories*

Transport phenomena in magnetic materials are in general discussed in the framework of two simplifying models (Rossiter 1987). The first is Matthiessen's rule that states that thermal and impurity scattering contribute independently to the electrical resistivity (see *Boltzmann Equation and Scattering Mechanisms*). The two-current model of Mott assumes that the scattering of electrons at impurities in a magnetized sample does not change the electron spin orientation relative to the

magnetization, and that the scattering is different for majority and minority spin electrons. This implies that there are two independent currents in a magnetic material with two corresponding subband resistivities, $\rho^{\uparrow}$ and $\rho^{\downarrow}$, that add up to the total resistivity according to

$$\frac{1}{\bar{\rho}} = \frac{1}{\rho^{\downarrow}} + \frac{1}{\rho^{\uparrow}} \tag{9}$$

This approach clearly ignores spin-mixing, e.g., due to finite temperature magnon scattering. This effect is sometimes considered by introducing a parameter $\rho^{\uparrow\downarrow}$ that represents the rate of spin-flip transitions leading to (Fert and Campbell 1968)

$$\bar{\rho} = \frac{\rho^{\downarrow}\rho^{\uparrow} + \rho^{\uparrow\downarrow}(\rho^{\downarrow} + \rho^{\uparrow})}{\rho^{\downarrow} + \rho^{\uparrow} + 4\rho^{\uparrow\downarrow}} \tag{10}$$

The AMR originates from the different scattering rate of electrons that travel parallel or perpendicular to the direction of the magnetization. This is ascribed in general primarily to the spin–orbit coupling. Accordingly, it has been suggested that the AMR ratio can be expressed by (Campbell 1970)

$$\frac{\Delta\rho}{\bar{\rho}} = \gamma(\alpha - 1) \quad \text{with} \quad \alpha = \frac{\rho^{\downarrow}}{\rho^{\uparrow}} \tag{11}$$

where γ, primarily determined by spin–orbit coupling, describes the anisotropy of the spin-resolved resistivities according to

$$\rho_{\parallel}^{\uparrow} = \rho_{\perp}^{\uparrow} + \gamma\rho_{\perp}^{\downarrow}, \quad \rho_{\parallel}^{\downarrow} = \rho_{\perp}^{\downarrow} + \gamma\rho_{\perp}^{\uparrow} \tag{12}$$

In practice one determines the subband resistivities $\rho^{\uparrow(\downarrow)}$ and their ratio α indirectly by measuring deviations from Matthiessen's rule for the temperature dependence of the resistivity or for ternary alloys. The applicability of this model is shown in Fig. 3. Here experimental AMR ratios for various dilute nickel alloys are plotted as a function of experimental values for α. Obviously, the data approximately lie on a straight line given by Eqn. (11), if γ is chosen appropriately. However, for alloys for which α is close to unity, pronounced deviations from the behavior shown in Fig. 3 occur. Moreover, first-principles calculations have shown that the measured α is greatly reduced in comparison with values calculated on the basis of the two-current model because spin-mixing mechanisms are always present in real materials. These have been sometimes accounted for by using an extended version of Eqn. (11) (Campbell *et al.* 1970):

$$\frac{\Delta\rho}{\bar{\rho}} = \gamma\frac{(\rho^{\downarrow} - \rho^{\uparrow})\rho^{\downarrow}}{\rho^{\uparrow}\rho^{\downarrow} + \rho^{\uparrow\downarrow}(\rho^{\uparrow} + \rho^{\downarrow})} \tag{13}$$

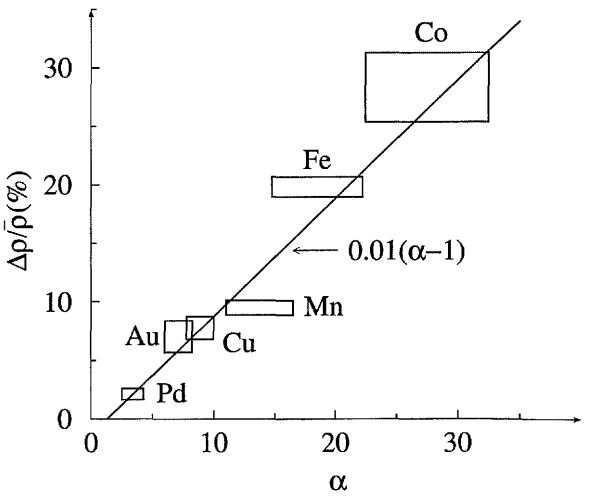

Figure 3
AMR ratio for various dilute nickel alloys NiX, with X = Pd, Au, Cu, Fe, Co (Campbell *et al.* 1970).

5. *Quantitative Models*

The first step towards a quantitative description of AMR was the combination of the model described above with a calculation of the residual electrical resistivity of disordered alloys on the basis of Mott's two-current model (Akai 1977). This questionable approximation could be avoided by the development of a fully relativistic description for the AMR effect (Banhart and Ebert 1995). The starting point of this approach is the formulation of the conductivity tensor as a current–current–correlation function within the Kubo–Greenwood response formalism (Edwards 1958):

$$\sigma_{\mu\mu} = \frac{\hbar}{\pi V_{\text{cryst}}} Tr\langle j_{\mu}\,\mathrm{Im}G^{+}(E_{\mathrm{F}})\,j_{\mu}\,\mathrm{Im}G^{+}(E_{\mathrm{F}})\rangle_{\text{conf}} \tag{14}$$

A similar but somewhat more complex expression can be given for the off-diagonal elements $\sigma_{\mu\nu}$. In Eqn. (14) the underlying electronic structure of the system is described by the retarded electronic Green's function $G^{+}(E_{\mathrm{F}})$ for the Fermi energy E_{F} (Butler 1985). In practice, this is calculated by means of multiple scattering theory.

Model calculations based on Eqn. (14) with the spin–orbit coupling manipulated reveal the role of this relativistic effect for AMR. Its major effect is to mix the minority and majority spin systems. As a consequence the two-current model in its strict sense is obviously not applicable. For the isotropic resistivity $\bar{\rho}$ it nevertheless gives reasonable results if the spin polarization at the Fermi level is not too high. This applies, for example, for the alloy systems Co_xPd_{1-x} and Co_xPt_{1-x}, while for Fe_xNi_{1-x} inclusion of the spin–orbit coupling increases $\bar{\rho}$ by up to an order of

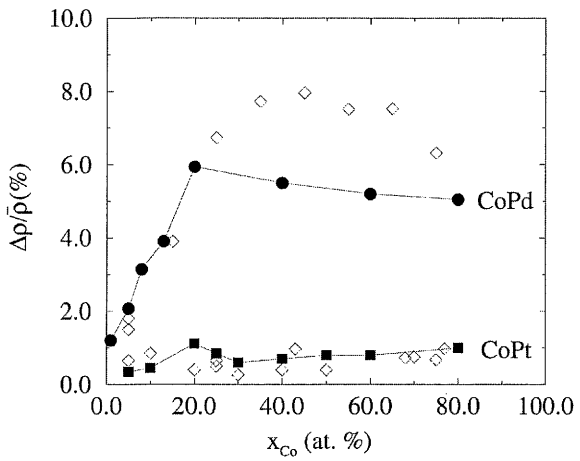

Figure 4
AMR ratio $\Delta\rho/\bar{\rho}$ for the alloy systems Co_xPd_{1-x} and Co_xPt_{1-x} at $T = 0$ K calculated by means of Eqn. (14) (filled symbols) and compared to experimental data (Ebert *et al.* 1996).

magnitude compared to a calculation based on the two-current model. The model calculations also demonstrate that the AMR effect is indeed caused by the spin–orbit coupling with AMR increasing quadratically with its strength. In addition it is found that the spin–orbit coupling causes AMR nearly exclusively via the mixing of the spin systems. This implies in particular that contributions to the AMR due to the spin-diagonal part of the spin–orbit coupling can be neglected.

Use of the formalism described above leads for the conductivity tensor automatically to the structure given by Eqn. (1) that is required from symmetry considerations. As an example of its application, Fig. 4 shows results for the AMR ratio obtained for the alloy system Co_xPd_{1-x} and Co_xPt_{1-x} (without manipulating the spin–orbit coupling). The satisfying agreement implies that other possible sources of AMR, e.g., magnon scattering processes, can be neglected. Equation (14) has been exploited only to account for the residual resistivity caused by the chemical disorder in alloys. However, it also allows the incorporation of other mechanisms and supplies an appropriate basis to deal with the temperature dependency of AMR.

6. *Summary*

The AMR effect is a galvanomagnetic effect, which can be observed in any spontaneously magnetized material. Most experimental work that aimed to optimize the AMR ratio of materials applied in sensor and storage technology has been focused on transition metal alloys. For these systems, values for the AMR ratio of up to 30% have been found at low temperatures, with only a few percent remaining at room temperature.

A phenomenological description of the AMR effect is obtained by assuming an anisotropy in the transport properties, represented by a corresponding conductivity tensor. This anisotropy can primarily be ascribed to the presence of the spin–orbit coupling and the magnetic ordering. Starting from this, microscopic descriptions of the AMR effect have been developed. Most of this theoretical work has been based on Mott's two-current model together with the use of some parameters. Modern *ab initio* band structure calculations allow parameter-free calculations of AMR. Corresponding investigations essentially confirm the ideas of the previous more phenomenological work and supply a very detailed understanding for the physical mechanisms giving rise to AMR.

See also: Giant Magnetoresistance: Metamagnetic Transitions in Metallic Antiferromagnets; Magnetoresistance: Magnetic and Nonmagnetic Intermetallic; Giant Magnetoresistance: Metamagnetic Transitions in Metallic Antiferromagnets; Giant Magnetoresistance

Bibliography

Akai H 1977 *Physica B* **86–88**, 539–40
Banhart J, Ebert H 1995 *Europhys. Lett.* **32**, 517–22
Becker R, Döring W 1939 *Ferromagnetismus*. Springer-Verlag, Berlin
Butherus A D, Nakahara S 1985 *IEEE Trans. Magn.* **21**, 1301–5
Butler W H 1985 *Phys. Rev. B* **31**, 3260–77
Campbell I A 1970 *Phys. Rev. Lett.* **24**, 269–71
Campbell I A, Fert A, Jaoul O 1970 *Physica C* **3**, S95–101
Cracknell A P 1973 *Phys. Rev. B* **7**, 2145–54
Dorleijn J W F 1976 *Philips Res. Rep.* **31**, 287–410
Ebert H, Banhart J, Vernes A 1996 *Phys. Rev. B* **54**, 8479–86
Edwards S F 1958 *Phil. Mag.* **3**, 1020–31
Eijkel K J M, Fluitman J H J 1990 *IEEE Trans. Magn.* **26**, 311–21
van Elst H C 1959 *Physica* **25**, 708–20
Fert A, Campbell I A 1968 *Phys. Rev. Lett.* **21**, 1190–2
Freitas P P, Plaskett T S 1990 *Phys. Rev. Lett.* **64**, 2184–7
Göpel W, Hesse J, Zemel J N (eds.) 1989 *Magnetic Sensors*. VCH, Weinheim, Germany
Karplus R, Luttinger J M 1954 *Phys. Rev.* **95**, 1154–60
Kleiner W H 1966 *Phys. Rev.* **142**, 318–26
McGuire T R, Potter R I 1975 *IEEE Trans. Magn.* **11**, 1018–38
Rossiter P L 1987 *The Electrical Resistivity of Metals and Alloys*. Cambridge University Press, Cambridge, UK
Smit J 1951 *Physica* **16**, 612–27
Smit J 1955 *Physica* **21**, 877–87
Wijn H P J (ed.) 1991 *Magnetic Properties of Metals d-Elements, Alloys and Compounds*. Springer-Verlag, Berlin

H. Ebert, A. Vernes, and J. Banhart